The American Journal of Human Genetics, Volume *105*

Supplemental Data

De Novo Mutations in *FOXJ1* Result in a Motile Ciliopathy with Hydrocephalus and Randomization of Left/Right Body Asymmetry

Julia Wallmeier, Diana Frank, Amelia Shoemark, Tabea Nöthe-Menchen, Sandra Cindric, Heike Olbrich, Niki T. Loges, Isabella Aprea, Gerard W. Dougherty, Petra Pennekamp, Thomas Kaiser, Hannah M. Mitchison, Claire Hogg, Siobhán B. Carr, Maimoona A. Zariwala, Thomas Ferkol, Margaret W. Leigh, Stephanie D. Davis, Jeffrey Atkinson, Susan K. Dutcher, Michael R. Knowles, Holger Thiele, Janine Altmüller, Henrike Krenz, Marius Wöste, Angela Brentrup, Frank Ahrens, Christian Vogelberg, Deborah J. Morris-Rosendahl, and Heymut Omran

Supplemental Figures:

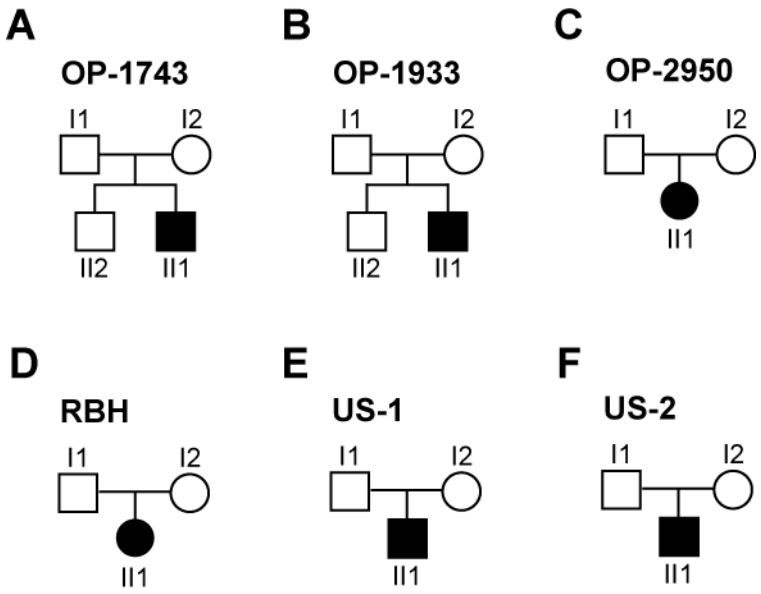

Figure S1:

Pedigrees of the families OP-1743, OP-1933, OP-2950, RBH, US-1 and US-2.

Consistent with *de novo* mutations neither the parents nor unaffected siblings are affected or carriers of the *FOXJ1* variants. For US-2, parental DNA was not available.

Gene	Gene ID	Control 1	Control 2	OP-2950 II1	OP-1743 II1
FOXJ1	NM_001454.3	74.46633826	68.21734089	29.39850001	3.215332057
SPAG1	NM_003114.4	0.828390805	1.024705467	0.433318857	0.463758765
C21ORF59	NM_021254.2	13.06333333	7.189811936	6.496993335	3.247919024
DNALI1	NM_003462.3	20.43285714	17.14633368	6.331309403	1.366886311
DNAH5	NM_001369.2	16.53530378	13.20986202	10.59849333	0.607105461
DNAH11	NM_001277115.1	3.115615764	2.054940253	1.213322866	0.190381503
CCDC103	NM_001258395.1	0.411559934	0.414682106	0.187298512	0.012491142
CCDC114	NM_144577.3	2.801970443	1.507537688	0.583819132	0.053581816
ARMC4	NM_001290020.1	0.297914614	0.341574091	0.105417008	0.014521878
CCDC151	NM_001302453.1	0.771609195	0.786322919	0.324619573	0.000000000
CCDC39	NM_181426.1	10.03284072	6.319221526	2.263350427	0.243265254
CCDC40	NM_017950.3	2.833858785	2.189156485	0.921024939	0.049710726
GAS8	NM_001286205.1	0.608390805	0.671181997	0.40311858	0.114345246
RSPH9	NM_152732.4	3.534909688	3.750474782	2.806387492	0.017652596
RSPH4A	NM_001161664.1	13.10172414	13.57083074	2.173100372	0.166541508
RSPH1	NM_080860.3	13.38555008	9.462933396	5.7530526	0.395570457
DNAJB13	NM_153614.3	0.690755337	0.83721282	0.468212872	0.042423345
HYDIN	NM_001270974.2	10.83711002	5.668644224	6.560492425	0.469100024
MNS1	NM_018365.2	38.11165846	32.04988151	11.12465966	1.057675019
PTK2	NM_001199649.1	1.635730706	1.035528815	0.779536305	1.456809841
CEP164	NM_014956.4	2.741724138	1.959563705	1.447341607	2.175330788

Figure S2:

Air-liquid interface (ALI-) cultured *FOXJ1* mutant respiratory epithelial cells show reduced transcript levels for *FOXJ1* and direct target genes.

3´mRNA-seq was performed with RNA extracted from ALI-cultured respiratory epithelial cells from controls and *FOXJ* mutant individuals (OP-1743 II1, OP-2950 II1) 15 days after airlift. Raw RNA-sequencing data were normalized against *GAPDH*. OP-1743 II1 and OP-2950 II1 show reduced transcript levels for *FOXJ1* and direct target genes in comparison to controls consistent with haploinsufficiency in *FOXJ1* mutant cells. The transcript levels for PTK2 and CEP164 are heterogenous.

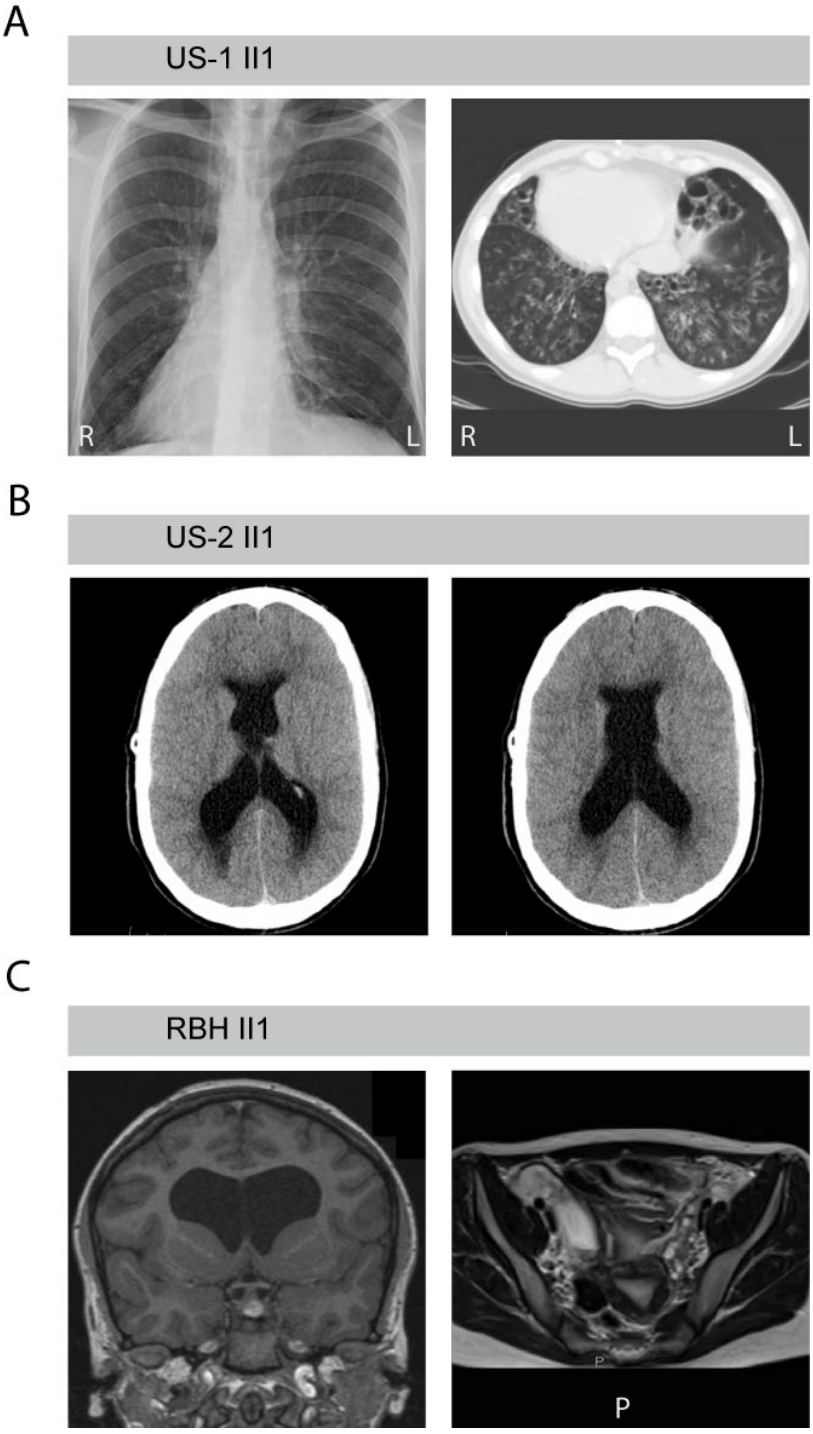

Figure S3:

***FOXJ1* mutant individuals showing bronchiectasis, randomization of left/right body asymmetry, obstructive hydrocephalus and hydrosalpinx.**

(**A**) Chest X-ray of US-1 II1 shows *situs inversus totalis.* The computed tomography scan (CT) of US-1 II1 exhibits bronchiectasis of the middle lobe. (**B**, **C**) Brain CT scan of individual US-2 II1 and coronar cranial magnetic resonance imaging scan (MRI) of RBH II1 showing enlarged lateral ventricles. (**C**) Pelvic MRI of RBH II1 at the age of 15 years exhibits distended fallopian tubes due to fluid accumulation.

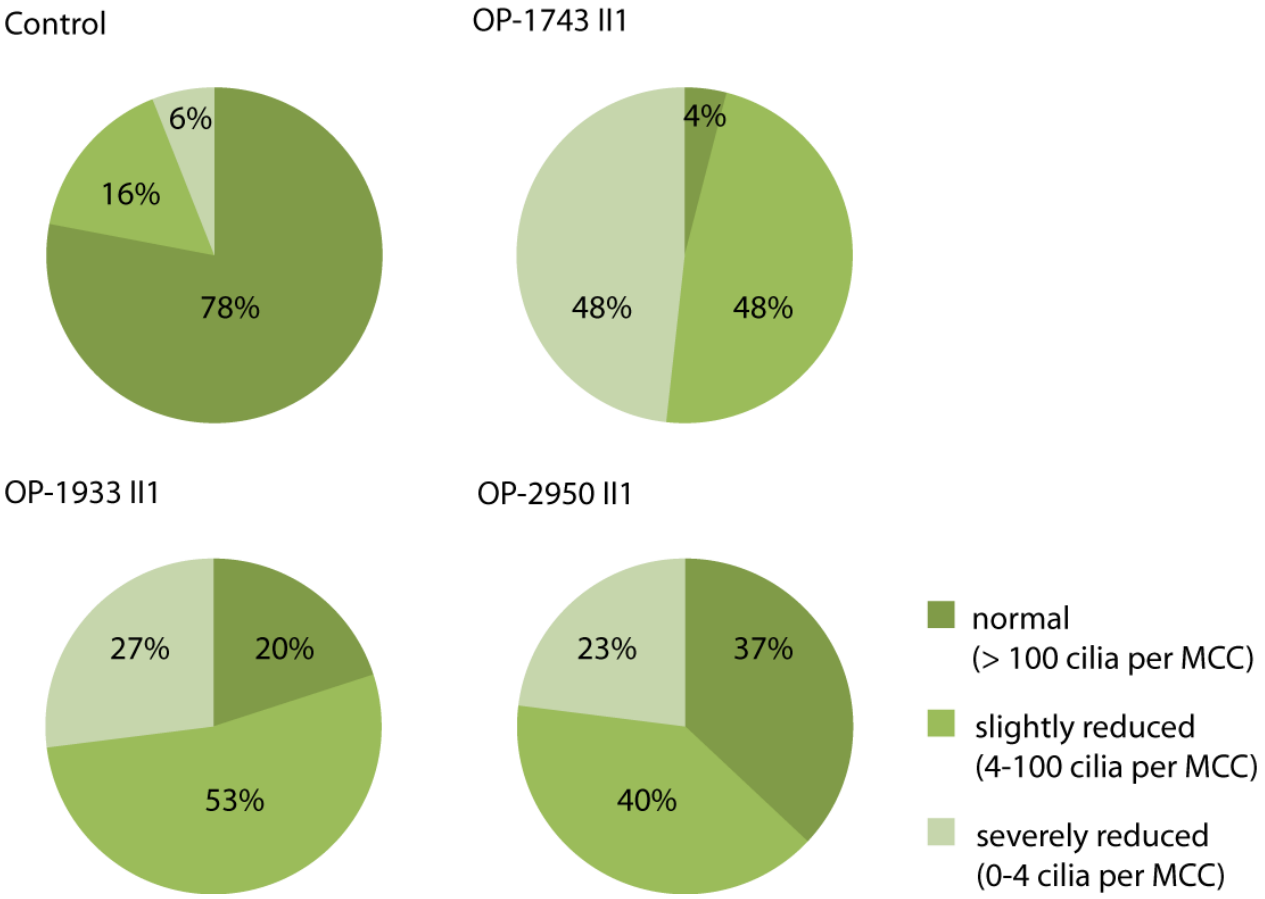

Figure S4:

***FOXJ1* mutant respiratory epithelial cells show variable numbers of cilia per multiciliated cell (MCC).**

Heterogeneous numbers of cilia of *Foxj1* mutants cells are evaluated by classifying into the categories: normal (>100 cilia per MCC), slightly reduced (4-100 cilia per MCC) and severely reduced (0-4 cilia per MCC). Whereas 78% of the control cells are normally ciliated, the number of normal ciliated cells of *Foxj1* mutant cells is greatly reduced. For the control, OP-1933 II1 and OP-2950 II1 100 cells per individual were evaluated. For OP-1743 II1 80 cells were analyzed.

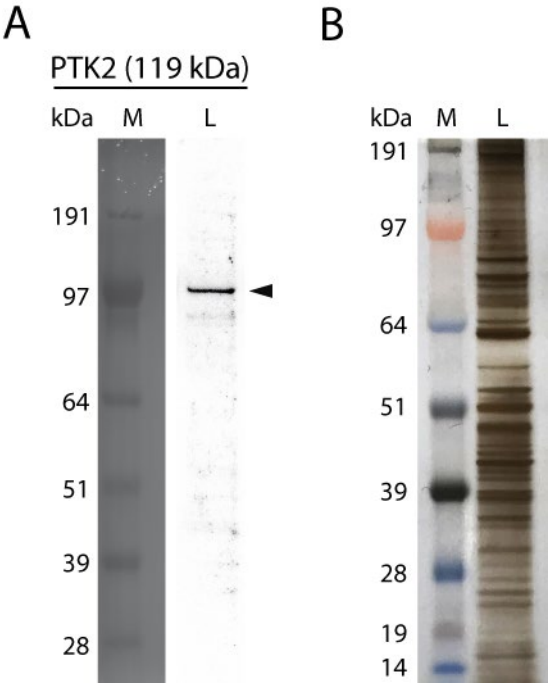

Figure S5:

Western blot analysis with monoclonal antibodies directed against PTK2.

(**A**) Western blot analysis confirming specificity of the mouse monoclonal antibody directed against PTK2 (protein tyrosine kinase 2). A correct sized band around 119 kDa (PTK2) is marked. (**B**) The protein content of the protein lysate was verified by silver staining. (M: marker; L: lysate extracted from control respiratory epithelial cells cultured under air-liquid interface condition)

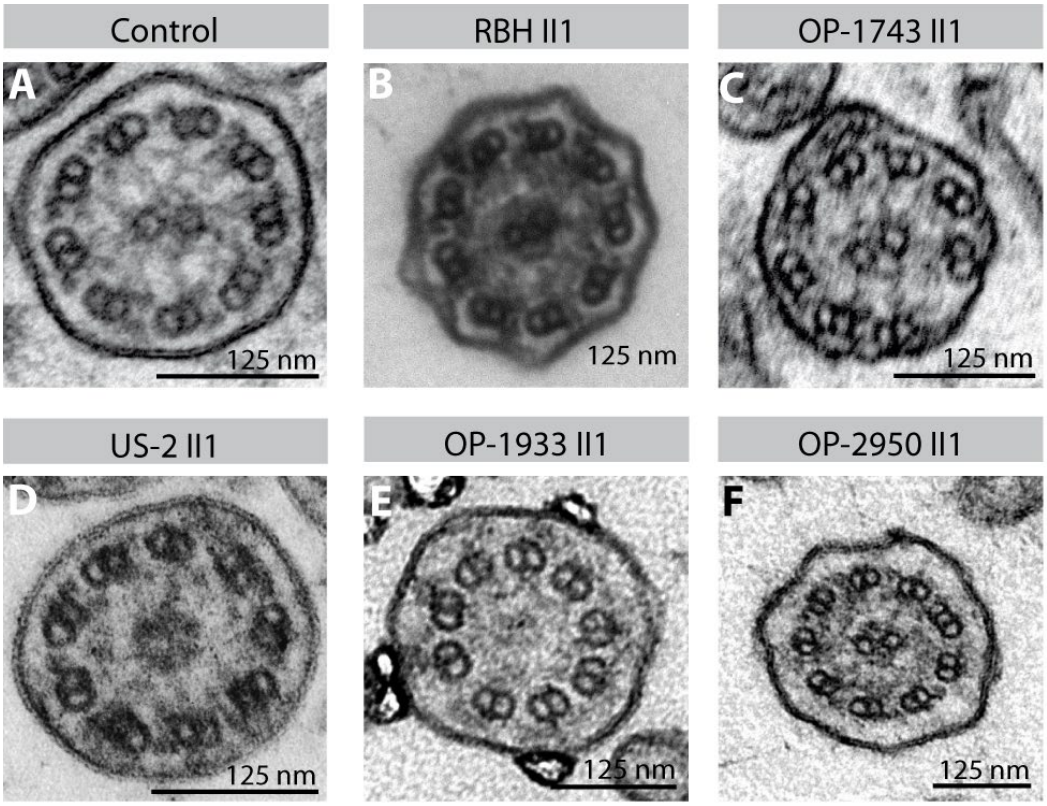

	ciliary cross sections (total)	A+B normal axonemal structure	C microtubular disorganization	D+E missing central pair	E+F reduced number of ODAs
RBH II1	163	65.6%	22.7%	4.9%	6.7%
OP-1933 II1	18	16.7%	0%	83.3%	0%
OP-2950 II1	12	33.2%	8.3%	25.0%	33.3%
US-1 II1	62	69.4%	3.2%	27.4%	n/a
US-2 II1	79	67.1%	8.9%	24.1%	n/a
Mean		50.4%	8.6%	32.9%	13.3%
Range		16.7 - 69.4%	0 - 22.7%	4.9 - 83.3%	0 - 33.3%

Figure S6:

Ciliary cross sections of *FOXJ1* mutant respiratory epithelial cells show variable structural defects by transmission electron microscopy (TEM).

By transmission electron microscopy (TEM) analyses, cross sections of *Foxj1* mutant cilia show in addition to normal ciliary cross sections (50.4%; **A, B**) heterogeneous defects including defective tubular organization (8.6%; **C**), missing central pair (32.9%; **D, E**) and reduced number of outer dynein arms (ODAs;13.3%; **E, F**). Left column represents the total number of ciliary cross sections counted per individual.

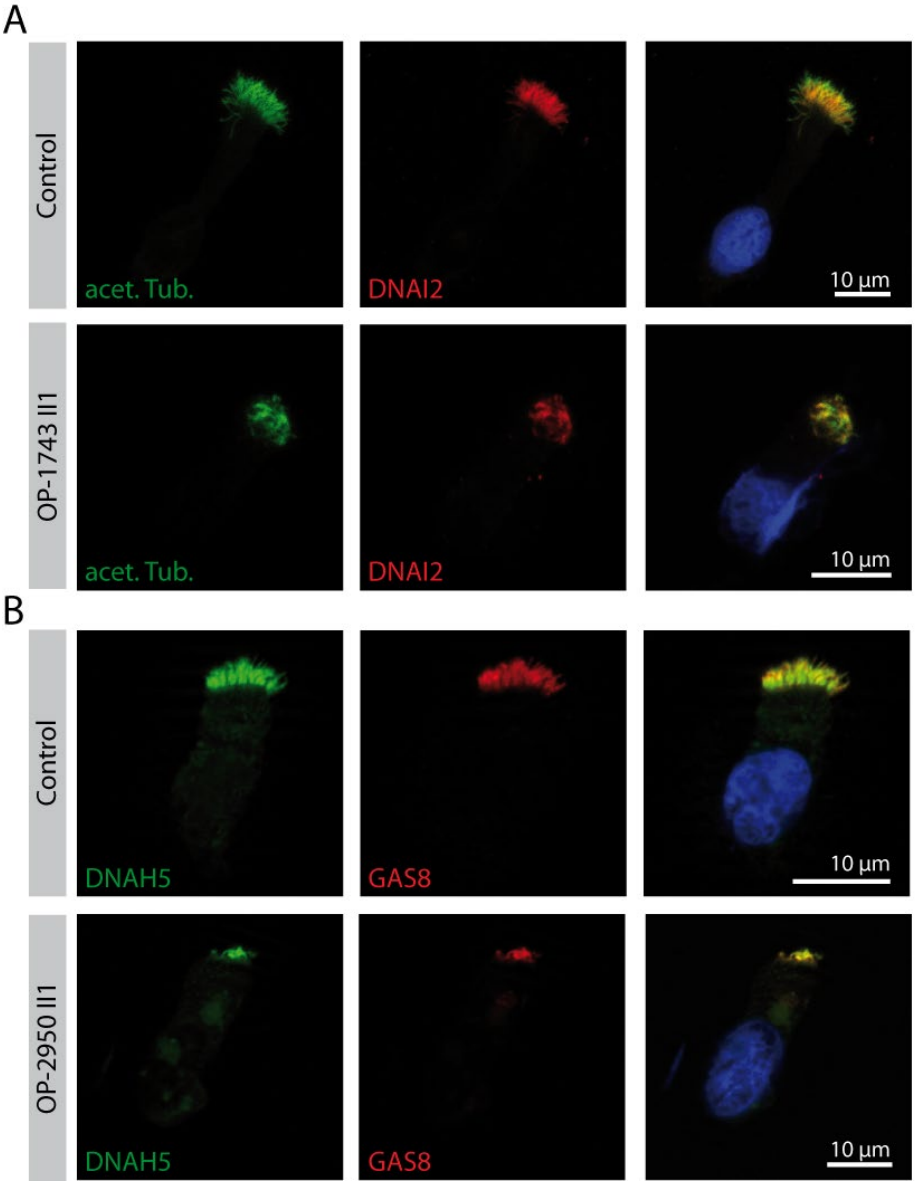

Figure S7:

Analysis of ciliary axonemal components in multiple motile cilia of *FOXJ1* mutant respiratory epithelial by Immunofluorescence microscopy analysis (IF).

(**A**) Immunofluorescence microscopy analysis (IF) with *Foxj1* mutant respiratory epithelial cells using antibodies directed against the outer dynein arm component DNAI2 (red) demonstrates co-localization with acetylated α-tubulin (acet. Tub.; green) along the whole cilium in control cells (demonstrated by yellow color in merge image). For the *Foxj1* mutant respiratory epithelial cell (OP-1743 II1), acetylated α-tubulin co-localizes with DNAI2, consistent with a normal expression and localization of DNAI2, whereas the number of cilia per cell is severely reduced. (**B**) The outer dynein arm heavy chain DNAH5 (green) and the nexin link-dynein regulatory complex component GAS8 (red) co-localize along the entire cilium (yellow) in the control as well as in the *Foxj1 mutant* (OP-2950 II1) respiratory epithelial cells. However, *Foxj1 mutant* cells demonstrate a reduced number of cilia. Nuclei were stained with Hoechst33342 (blue).

Supplemental Methods:

Individuals. Based on approved protocols from the Institutional Ethics Review Board of the University Muenster, Freiburg and collaborating institutions, we obtained signed and informed consent from all affected individuals and relatives. Patient RBH II1 and her parents were recruited to the UK 100,000 Genomes Project. Study participants from US-1 and US-2 families were recruited at the University of North Carolina at Chapel Hill (UNC) and the collaborating site of Genetic Disorders of Mucociliary Clearance Consortium (GDMCC) and signed informed consents were obtained. The study was approved by the institutional review board for the protection of the Rights of Human Subjects at the UNC and collaborating institution.

Whole Exome Sequencing. Genomic DNA was directly extracted from blood by standard protocols and sent to the Cologne Center for Genomics for targeted-exome sequencing. Whole exome sequencing was performed as described in Altmüller *et al.*[1]. Variants representing a minor-allele frequency greater than / or equal 0.01 in the genome aggregation database (gnomAD) were neglected. Whole exome sequencing for the probands from the US-1 and US-2 families were carried out at the McDonnell Genome Institute (St. Louis) using the XGen Exome Research panel v1.0 probe set (Integrated DNA Technologies). Variants were annotated using Ensembl Variant Effect Predictor. All of the variants in the 44 genes currently known to be associated with PCD and/or motile ciliopathies; and *FOXJ1*[2,3], were extracted from the WES dataset for the manual review. High frequency variants (>= 0.01 minor allele frequency in gnomAD) were filtered out and the remaining variants were carefully assessed based on the ACMG guidelines[2].*FOXJ1* variant confirmation and segregation analysis (where possible) was carried out using Sanger sequencing.

Whole Genome Sequencing. Whole genome sequencing datasets were created through the UK 100,000 Genomes Project main program, using Illumina X10 sequencing chemistry. Sequencing reads were aligned to build GRCh37 of the human reference genome utilizing Issac (Aligner). Small variants were identified through Starline (SNV and small indels ≤ 50bp), and structural variants were identified utilizing Manta and Canvas (CNV Caller). Variants were annotated and analyzed with the Ensembl variant effect predictor (v92) and bespoke perl scripts within the Genomics England secure research embassy. Virtual gene panels were applied to the analysis according to pedigree information and HPO terms submitted with the patient. Variants were tiered according to the Project Tiering algorithm as follows: predicted most-severe rare variants in a gene in the virtual gene panel (Tier 1), other rare, protein-altering variants in known disease genes (Tier 2) and potentially pathogenic rare variants in any other genes (Tier 3). Tier 3 variants were assessed in the Clinical Genetics and Genomics Laboratory, RBHT, according to in-house bioinformatic pipelines for variant assessment according to the ACMG guidelines[4].Technical validation of the *FOXJ1* variant c.967delG was performed in the patient and checked in her parents by Sanger sequencing of the entire coding region of the gene.

Cultivation of respiratory epithelial cells. Respiratory epithelial cells were obtained from the middle turbinate by nasal brush biopsies (Engelbrecht Medicine and Laboratory technology) and suspended in cell culture medium. Cells were pre-cultured in rat collagen-coated cell culture flasks and subsequently processed as previously reported to spheroids[5] or to air-liquid interface (ALI-) cultures[6,7]. As cell culture medium

PneumaCult™-Ex Medium (Stemcell™) for proliferation and PneumaCult™-ALI Medium (Stemcell™) for differentiation supplied with 1% Antibiotic - Antimycotic 100x (gibco®) was used for ALI-cultures.

3´mRNA Sequencing. RNA was extracted from ALI-cultured respiratory epithelial cells 15 days after airlift using the RNeasy Minit Kit (Quiagen). RNA was sent to the Cologne Center for Genomics for 3´mRNA sequencing. Library preparation was performed using the QuantSeq 3´mRNA-Seq Library Prep Kit for Illumina (FWD; Lexogen) following the manufactory protocol. Sequencing was performed on the Illumina platform. Raw data were analyzed using bioinformatic programs available on galaxy[8]. Reads were trimmed as recommended using the program Trim sequences (Assaf Gordon (2010). FASTQ/A short-reads pre-processing tools. http://hannonlab.cshl.edu/fastx_toolkit/). Trimmed files were aligned and quantified using the program Salmon[9]. As reference the transcriptome GRch37latest.rna.fna_gz (https://www.ncbi.nlm.nih.gov/genome/guide/human/) was used. Counted reads of transcript variants of interest were normalized against g*lyceraldehyde 3-phosphate dehydrogenase* (*GAPDH).*

HVMA (high speed video microscopy). Human respiratory epithelial cells were analyzed as previously described[10].

Particle tracking. Respiratory epithelial cells cultured under ALI-conditions were used for tracking experiments. In total, two ALI-Transwell® inserts per person (#1 and #2) were tracked three times (day 30, day 37 (data here not shown) and day 44 after airlift). First, secreted mucus was removed by washing the apical compartment with Dulbecco's Phosphate-Buffered Saline (DPBS; without Mg^{2+}/Ca^{2+}). In a second step cultures were equilibrated for 20 min on the heating plate (37°C) of a Nikon Eclips Ti-S microscope. Afterwards, 100 µl cell culture medium was added to the apical compartment of the Transwell® inserts for 10 min on the heating plate (37°C). 10 µl of a fluorescent beads stock solution (FluoSpheres® 0.5 µm in diameter; Thermo Fisher, diluted 1:1,000 in DPBS without Mg^{2+}/Ca^{2+}) were mixed with 90 µl pre-warmed cell culture medium and added to the apical compartment of the Transwell® insert as well. Transport of fluorescent nanoparticles by ciliary beating was recorded using the Nikon Eclips Ti-S microscope (20x objective lens) equipped with the NIS-Elements Advanced Research software (20 sec; 7.5 frames per second). Nanoparticles were excited with a wavelength of 546 nm (100 ms exposure time). Tracking videos were evaluated using the NIS-Elements Advanced Research software (Version 4.51.000) and NIS Advanced 2D Tracking plug-in to generate polar graphs and to determine the speed (µm/s) as well as the mean square displacement ($µm^2$) per tracked particle. In total, 15 videos per individuals were analyzed for the statistical evaluation and thereby 253 particles were tracked per video on average. Z-stack projections of movies were generated using ImageJ. In parallel to each recorded tracking video, a corresponding differential interference contrast (DIC) video was taken by an additionally equipped Basler sc640-120fm monochrome high-speed video camera (recording 125 frames per second) to state the cells condition as well as the ciliary beating pattern. DIC videos were evaluated using SAVA software[11].

Transmission electron microscopy (TEM). Native as well as cultured respiratory epithelial cells were fixated in 2.5% glutaraldehyde and processed for TEM analyses by standardized protocols as previously reported[12–14].

Sections were collected on copper grids, stained with Reynold´s lead citrate and visualized using the Philips CM10 or Jeol 1400+.

High-resolution immunofluorescence microscopy (IF). Native or as spheroids cultured respiratory epithelial cells were spread onto glass-slides and air-dried. Excess medium was removed with 1x phosphate-buffered saline (PBS). The cells were treated with 4% paraformaldehyde, 0.2% Trition X-100/1x PBS and 1% skim milk-blocking solution (in 1x PBS). Primary antibody incubation (antibodies were diluted in blocking solution) was performed overnight at 4°C. Mouse monoclonal antibodies against DNAH5 were previously reported[15]. Mouse monoclonal antibodies directed against acetylated α-tubulin (1:10,000; T6793) were obtained from Sigma. The rabbit polyclonal antibodies against DNAI2 (1:500; HPA050565)[16], CEP164 (1:500; HPA037605), RSPH4a (1:400; HPA031196)[17] and GAS8 (1:500; HPA041311)[18] were purchased from Atlas Antibodies. Mouse monoclonal PTK2 antibody (1:200; clone 4.47, 05-537) was obtained from Upstate. The following incubation of the secondary antibodies, including Alexa Fluor 488-conjugated goat antibodies to mouse (1:1,000; A11029; Invitrogen) and Alexa Fluor 546-conjugated goat antibodies to rabbit (1:1,000; A11035; Invitrogen), was carried out for 30 min at room temperature. Nuclei were stained with Hoechst 33342 (1:1,000 in 1x PBS; 14533-100MG, Sigma). Immunofluorescence images were taken using a Zeiss Apotome Axiovert 200 and processed with AxioVersion 4.8. or a Zeiss LSM 880 Laser Scanning Microscope and corresponding ZEN-blue and ZEN-black software programs for processing were used to prepare confocal images. Adobe Creative Suites were used for final image processing.

Immunoblotting. Proteins were extracted from nasal epithelial cells of healthy volunteers cultured under ALI-conditions after complete differentiation using the following buffer: 50 mM Tris-HCl (pH 8.0), 150 mM NaCl, 1% IGEPAL, 10% Glycerol, and 0.5 mM EDTA supplemented with cOmplete™ Mini EDTA-free Protease Inhibitor Cocktail Tablets (Roche) and Phosphatase Inhibitor Cocktails 2 and 3 (Sigma-Aldrich). Using the Mikro-Dismembrator U (Sartorius), cell lysates were homogenized (2,000 rpm, 3 min) and proteins were separated from residual cell components by a final centrifugation step (11,500 rpm; 20 min; 4°C). Soluble fractions were recovered and mixed with dithiotriol (DTT) and lithium dodecyl sulfate (LDS) buffer (10 µl lysate, 5 µl NuPAGE® 4x LDS sample buffer (novex® by life technologies), 2 µl 1 M DTT, 3 µl water) and heated for 10 min at 70°C. To gauge the protein content of the cell lysate, proteins were separated in a NuPAGE® 4-12 % Bis-Tris gel (Invitrogen) and stained by silver staining using the Proteo Silver™ Silver Stain kit (Prot-SIL1, Sigma) according to the manufacture's protocol. For immunoblotting, proteins were electrophoresed in a NuPAGE® 4-12% Bis-Tris gel and transferred to an Invitrolon™ polyvinylidene difluoride (PVDF)-membrane (novex® by life technologies). PVDF-membrane was washed two times (5 min each) with Tris-buffered saline plus Tween 20 (TBST) and blocked in 5 % skim milk in TBST overnight at 4°C. The mouse monoclonal primary antibodies against PTK2 (1:1,000; clone 4.47, 05-537, Upstate) were diluted in 1% skim milk in TBST and incubated with the membranes for 4 h at room temperature. After washing with TBST four times (7.5 min each) at room temperature, the membrane was incubated with secondary goat anti-mouse HRP antibody (1:3,000 diluted in 1% skim milk in TBST; NA931V, GE Healthcare) for 1 h at room temperature. The membrane was washed additional eight times (7.5 min. each) with TBST before performing the enhanced chemoluminescence

(ECL) step using Prime Western Blotting Detection Reagent (GE Healthcare). Digital images were acquired using a FUSION-SL Advance Imager (PeqLab). Using Adobe Photoshop v. CS4 (Adobe), the contrast of the images were optimized.

Acknowledgement:

This work was supported by the Deutsche Forschungsgemeinschaft WA 4283/1-1 to J.W., OM6/7, OM6/8, OM6/10, OM6/11 (CRU 326) and OM6/14-1 to H.O., OL450/1 (H.Ol.), IZKF Muenster to H.O. (Om2/009/12 and Om/015/16), “Innovative Medical Research“ of the University of Muenster Medical School to N.T.L. (I-LO121517) and WA 1 2 14 18 (J.W.), "Dekanat der Medizinischen Fakultät der WWU" (J.W)., NIH-NHLBI grant U54HL096458 to M.A.Z., S.D.D., M.W.L., T.W.L., J.J.A., and M.R.K., and NIH-NHLBI grant R01HL071798 to M.A.Z., and M.R.K., NIH-NHLBI grant R0H128370 to S.K.D. and NIH-NCATS grant UL1 TR000083 to UNC. R01 HL071798 and U54HL096458, funding received through a collaboration of NCATS and NHLBI. The authors participate in the COST action BEAT-PCD: Better Evidence to Advance Therapeutic options for PCD network (BM11407). H.M.M. acknowledges Great Ormond Street Children’s Charity (V1299, V2217) and the NIHR Great Ormond Street Hospital Biomedical Research Centre (GOSH BRC). The American authors were supported by the National Institutes of Health (NIH) Genetic Disorders of Mucociliary Clearance Consortium (HL096458), part of the NIH Rare Disease Clinical Research Network (RDCRN), supported through collaboration between NIH Office of Rare Diseases Research (ORDR) at the National Center for Advancing Translational Science (NCATS) and National Heart, Lung and Blood Institute (NHLBI). The findings in patient RBH II1 were made possible through access to the data and findings generated by the 100,000 Genomes Project. The 100,000 Genomes Project is managed by Genomics England Limited (a wholly owned company of the Department of Health). The 100,000 Genomes Project is funded by the National Institute for Health Research and NHS England. The Wellcome Trust, Cancer Research UK and the Medical Research Council have funded research infrastructure. The 100,000 Genomes Project uses data provided by patients and collected by the National Health Service as part of their care and support. The Genetics Disorders of Mucociliary Clearance Consortium (U54HL096458) is a part of the NCATS Rare Disease Clinical Research Network (RDCRN). RDCRN is an initiative of the Office of Rare Diseases Research (ORDR), NCATS, funded through a collaboration between NCATS and NHLBI. The contents are solely the responsibility of the authors and do not necessarily represent the official view of the National Institute of Health (NIH). Several authors of this publication are members of the European Reference Network for Rare Respiratory Diseases (ERN-LUNG) – Project ID No 739546.

References:

1. Altmüller, J., Motameny, S., Becker, C., Thiele, H., Chatterjee, S., Wollnik, B., and Nürnberg, P. (2016). A systematic comparison of two new releases of exome sequencing products: the aim of use determines the choice of product. Biol. Chem. *397*, 791–801.

2. Chen, J., Knowles, H.J., Hebert, J.L., and Hackett, B.P. (1998). Mutation of the mouse hepatocyte nuclear factor/forkhead homologue 4 gene results in an absence of cilia and random left-right asymmetry. J. Clin. Invest. *102*, 1077–1082.

3. Brody, S.L., Yan, X.H., Wuerffel, M.K., Song, S.K., and Shapiro, S.D. (2000). Ciliogenesis and left-right axis defects in forkhead factor HFH-4-null mice. Am. J. Respir. Cell Mol. Biol. *23*, 45–51.

4. Richards, S., Aziz, N., Bale, S., Bick, D., Das, S., Gastier-Foster, J., Grody, W.W., Hegde, M., Lyon, E., Spector, E., et al. (2015). Standards and guidelines for the interpretation of sequence variants: a joint consensus recommendation of the American College of Medical Genetics and Genomics and the Association for Molecular Pathology. Genet. Med. *17*, 405–424.

5. Olbrich, H., Horváth, J., Fekete, A., Loges, N.T., Storm van's Gravesande, K., Blum, A., Hörmann, K., and Omran, H. (2006). Axonemal localization of the dynein component DNAH5 is not altered in secondary ciliary dyskinesia. Pediatr. Res. *59*, 418–422.

6. Munye, M.M., Shoemark, A., Hirst, R.A., Delhove, J.M., Sharp, T. V, McKay, T.R., O'Callaghan, C., Baines, D.L., Howe, S.J., and Hart, S.L. (2017). BMI-1 extends proliferative potential of human bronchial epithelial cells while retaining their mucociliary differentiation capacity. Am. J. Physiol. Lung Cell. Mol. Physiol. *312*, L258–L267.

7. Hirst, R.A., Rutman, A., Williams, G., and O'Callaghan, C. (2010). Ciliated Air-Liquid Cultures as an Aid to Diagnostic Testing of Primary Ciliary Dyskinesia. Chest *138*, 1441–1447.

8. Afgan, E., Baker, D., Batut, B., van den Beek, M., Bouvier, D., Čech, M., Chilton, J., Clements, D., Coraor, N., Grüning, B.A., et al. (2018). The Galaxy platform for accessible, reproducible and collaborative biomedical analyses: 2018 update. Nucleic Acids Res. *46*, W537–W544.

9. Patro, R., Duggal, G., Love, M.I., Irizarry, R.A., and Kingsford, C. (2016). Salmon provides accurate, fast, and bias-aware transcript expression estimates using dual-phase inference. BioRxiv 021592.

10. Wallmeier, J., Al-Mutairi, D.A.D.A., Chen, C.-T.C.-T., Loges, N.T.N.T., Pennekamp, P., Menchen, T., Ma, L., Shamseldin, H.E.H.E., Olbrich, H., Dougherty, G.W.G.W., et al. (2014). Mutations in CCNO result in congenital mucociliary clearance disorder with reduced generation of multiple motile cilia. Nat. Genet. *46*, 646–651.

11. Sisson, J.H., Stoner, J.A., Ammons, B.A., and Wyatt, T.A. (2003). All-digital image capture and whole-field

analysis of ciliary beat frequency. J. Microsc. *211*, 103–111.

12. Wallmeier, J., Al-Mutairi, D.A., Chen, C.-T., Loges, N.T., Pennekamp, P., Menchen, T., Ma, L., Shamseldin, H.E., Olbrich, H., Dougherty, G.W., et al. (2014). Mutations in CCNO result in congenital mucociliary clearance disorder with reduced generation of multiple motile cilia. Nat. Genet. *46*,.

13. Shoemark, A., Dixon, M., Corrin, B., and Dewar, A. (2012). Twenty-year review of quantitative transmission electron microscopy for the diagnosis of primary ciliary dyskinesia. J. Clin. Pathol. *65*, 267–271.

14. Davis, S.D., Ferkol, T.W., Rosenfeld, M., Lee, H.-S., Dell, S.D., Sagel, S.D., Milla, C., Zariwala, M.A., Pittman, J.E., Shapiro, A.J., et al. (2015). Clinical features of childhood primary ciliary dyskinesia by genotype and ultrastructural phenotype. Am. J. Respir. Crit. Care Med. *191*, 316–324.

15. Omran, H., Kobayashi, D., Olbrich, H., Tsukahara, T., Loges, N.T., Hagiwara, H., Zhang, Q., Leblond, G., O'Toole, E., Hara, C., et al. (2008). Ktu/PF13 is required for cytoplasmic pre-assembly of axonemal dyneins. Nature *456*, 611–616.

16. Höben, I.M., Hjeij, R., Olbrich, H., Dougherty, G.W., Menchen, T., Aprea, I., Frank, D., Pennekamp, P., Dworniczak, B., Wallmeier, J., et al. (2018). Mutations in C11ORF70 Cause Primary Ciliary Dyskinesia with Randomization of Left/Right Body Asymmetry Due to Effects of Outer and Inner Dynein Arms. Am. J. Hum. Genet.

17. Frommer, A., Hjeij, R., Loges, N.T.N.T., Edelbusch, C., Jahnke, C., Raidt, J., Werner, C., Wallmeier, J., Große-Onnebrink, J., Olbrich, H., et al. (2015). Immunofluorescence Analysis and Diagnosis of Primary Ciliary Dyskinesia with Radial Spoke Defects. Am. J. Respir. Cell Mol. Biol. *53*, 563–573.

18. Olbrich, H., Cremers, C., Loges, N.T.N.T., Werner, C., Nielsen, K.G.K.G., Marthin, J.K.J.K., Philipsen, M., Wallmeier, J., Pennekamp, P., Menchen, T., et al. (2015). Loss-of-Function GAS8 Mutations Cause Primary Ciliary Dyskinesia and Disrupt the Nexin-Dynein Regulatory Complex. Am. J. Hum. Genet. *97*, 546–554.